Acta Medica Okayama

Volume 62, *Issue* 3 2008 *Article* 3

JUNE2008

Basic Study of Susceptibility-Weighted Imaging at 1.5T

Toshi Matsushita, *Department of Medical Radiotechnology, Okayama University Graduate School of Health Sciences*
Daigo Anami, *Divisions of Imaging Technology, Okayama Diagnostic Imaging Center*
Tadashi Arioka, *Divisions of Imaging Technology, Okayama Diagnostic Imaging Center*
Seiji Inoue, *Divisions of Imaging Technology, Okayama Diagnostic Imaging Center*
Yusuke Kariya, *Divisions of Imaging Technology, Okayama Diagnostic Imaging Center*
Masako Fujimoto, *Divisions of Imaging Technology, Okayama Diagnostic Imaging Center*
Kentaro Ida, *Divisions of Diagnostic Imaging, Okayama Diagnostic Imaging Center*
Nobuya Sasai, *Divisions of Diagnostic Imaging, Okayama Diagnostic Imaging Center*
Mitsumasa Kaji, *Divisions of Diagnostic Imaging, Okayama Diagnostic Imaging Center*
Susumu Kanazawa, *Department of Radiology, Okayama University Graduate School of Medicine, Dentistry and Pharmaceutical Sciences*
Ikuo Joja, *Department of Medical Radiotechnology, Okayama University Graduate School of Health Sciences*

Basic Study of Susceptibility-Weighted Imaging at 1.5T*

Toshi Matsushita, Daigo Anami, Tadashi Arioka, Seiji Inoue, Yusuke Kariya, Masako Fujimoto, Kentaro Ida, Nobuya Sasai, Mitsumasa Kaji, Susumu Kanazawa, and Ikuo Joja

Abstract

With the aim of sequence optimization in susceptibility-weighted imaging (SWI), 2 image acquisition parameters (slice thickness and matrix size) and 2 image processing conditions (number of slices per minimum intensity projection (MIP) and Sliding Window) were investigated using a 1.5-T magnetic resonance imaging (MRI) system. The subjects were 12 healthy volunteers and the target region for scanning was the whole brain. Informed consent was obtained from all subjects. First, susceptibility-weighted images were acquired with various slice thicknesses from 1mm to 5mm and various matrix sizes from 256x256 to 512x512, and the images were assessed in terms of the contrast-to-noise ratio (CNR) and were also visually evaluated by three radiologists. Then, the number of slices per MIP and the usefulness of the Sliding Window were investigated. In the study of the optimal slice thickness and matrix size, the results of visual evaluation suggested that a slice thickness of 3mm and a matrix size of 448x448 are optimal, while the results of evaluation based on CNR were not significant. As regards the image processing conditions, the results suggested that the number of slices per MIP should be set to a minimum value of 2 and that the use of Sliding Window is effective. The present study provides useful reference data for optimizing SWI sequences.

KEYWORDS: susceptibility, phase, contrast-to-noise ratio, number of slices per MIP, Sliding Window

---

PMID: 18596832

Acta Med. Okayama, 2008
Vol. 62, No. 3, pp. 159–168

Acta Medica Okayama
http://escholarship.lib.okayama-u.ac.jp/amo/

Original Article

Basic Study of Susceptibility-Weighted Imaging at 1.5T

Toshi Matsushita[a,b]*, Daigo Anami[b], Tadashi Arioka[b], Seiji Inoue[b], Yusuke Kariya[b], Masako Fujimoto[b], Kentaro Ida[c], Nobuya Sasai[c], Mitsumasa Kaji[c], Susumu Kanazawa[d], and Ikuo Joja[a]

[a]Department of Medical Radiotechnology, Okayama University Graduate School of Health Sciences, Okayama 700–8558, Japan,
Divisions of [b]Imaging Technology and [c]Diagnostic Imaging, Okayama Diagnostic Imaging Center, Okayama 700–0913, Japan, and
[d]Department of Radiology, Okayama University Graduate School of Medicine, Dentistry and Pharmaceutical Sciences, Okayama 700–8558, Japan

With the aim of sequence optimization in susceptibility-weighted imaging (SWI), 2 image acquisition parameters (slice thickness and matrix size) and 2 image processing conditions (number of slices per minimum intensity projection (MIP) and Sliding Window) were investigated using a 1.5-T magnetic resonance imaging (MRI) system. The subjects were 12 healthy volunteers and the target region for scanning was the whole brain. Informed consent was obtained from all subjects. First, susceptibility-weighted images were acquired with various slice thicknesses from 1 mm to 5 mm and various matrix sizes from 256 × 256 to 512 × 512, and the images were assessed in terms of the contrast-to-noise ratio (CNR) and were also visually evaluated by three radiologists. Then, the number of slices per MIP and the usefulness of the Sliding Window were investigated. In the study of the optimal slice thickness and matrix size, the results of visual evaluation suggested that a slice thickness of 3 mm and a matrix size of 448 × 448 are optimal, while the results of evaluation based on CNR were not significant. As regards the image processing conditions, the results suggested that the number of slices per MIP should be set to a minimum value of 2 and that the use of Sliding Window is effective. The present study provides useful reference data for optimizing SWI sequences.

Key words: susceptibility, phase, contrast-to-noise ratio, number of slices per MIP, Sliding Window

Susceptibility-weighted imaging (SWI) is an imaging technique that was developed by Haacke *et al.* in 2004 [1]. SWI exploits the phenomenon by which the phase and the change in the local magnetic field are proportional to each other if the echo time (TE) is constant. In SWI scans, data is acquired using a sequence of the 3D gradient echo type with flow compensation applied in 3 directions, and the magnitude image is then multiplied several times by the phase mask image, which is generated by filtering the phase image (Fig. 1) [1–3]. Conventionally, T2*-weighted imaging has been used to obtain susceptibility-weighted images in order to visualize hemorrhage and ferrugination in the head. SWI has dramatically improved the visualization not only of hemorrhage and ferrugination, but also of venous structures, permit-

Received November 21, 2007; accepted December 20, 2007.
*Corresponding author. Phone:+81-86-235-2511; Fax:+81-86-234-5633
E-mail:m-toshiy@okayama-dic.or.jp (T. Matsushita)

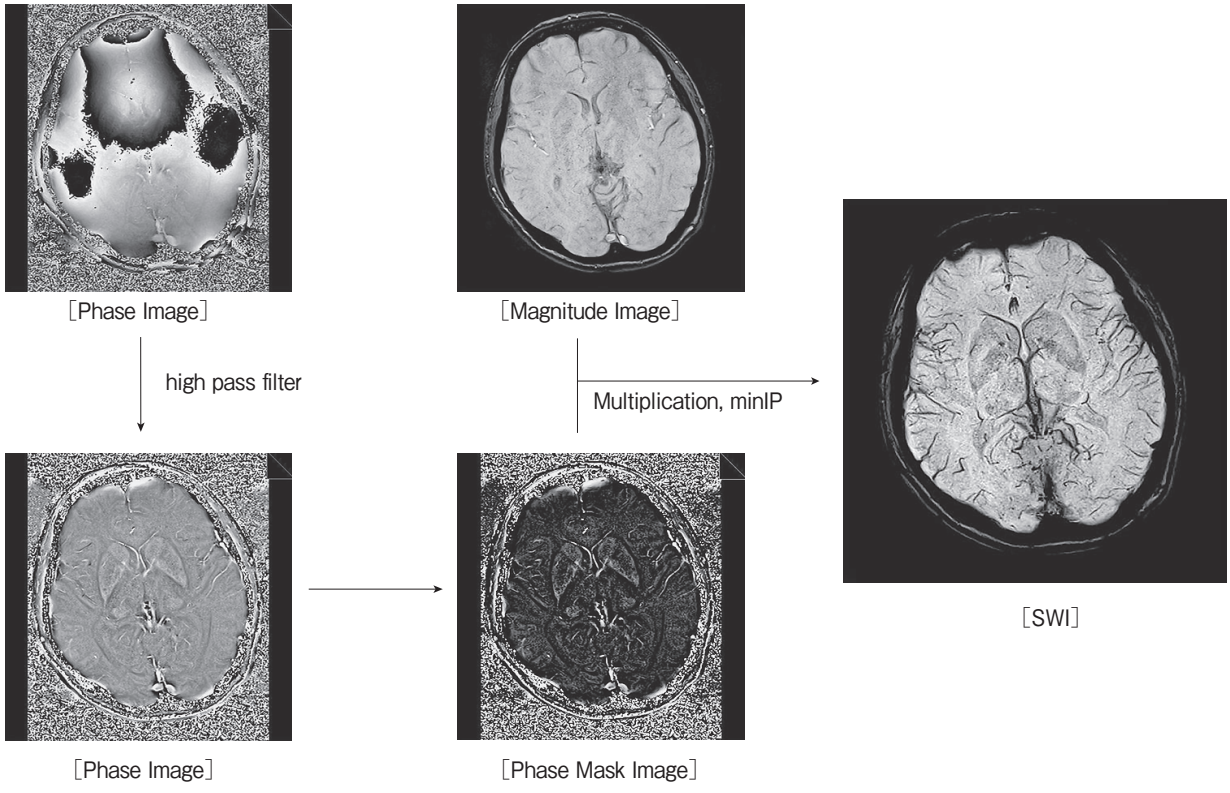

Fig. 1 Steps of image reconstruction in SWI.

ting smaller lesions to be depicted [4, 5]. SWI was originally intended to be used in 3-T MRI systems because its usefulness has been demonstrated for acquisition at higher resolutions, but there have been several discrepancies in reports regarding its use in 1.5-T systems [6]. However, there is insufficient basic data on SWI not only because it is a relatively new technique, but also because it is patented and therefore can be used in only a limited number of systems. Sequence optimization is essential when SWI is to be employed in clinical practice. In addition, the data acquired by SWI cannot be post-processed, and the image processing conditions must therefore be set prior to data acquisition. The present study was conducted to investigate imaging conditions and image processing conditions with the aim of optimizing the sequences employed for SWI in 1.5-T systems.

Materials and Methods

A 1.5-T MRI system (MAGNETOM Avanto, Siemens, Germany) and a head matrix coil were used for imaging. The target region for scanning was the whole brain, and the scanning range was set to 120 mm. Prior to the start of this study, approval was obtained from the ethics review board of the Okayama Diagnostic Imaging Center and informed consent to participate in the study was obtained from each volunteer.

Slice thickness and matrix size. One healthy volunteer (27-year-old male) underwent an SWI study with slice thickness variation from 1 to 5 mm in 1-mm steps, and the matrix size varied from 256×256 to 512×512 with isotropic pixels. Scan parameters other than slice thickness and matrix size are shown

Table 1 Scan parameters (physical evaluation based on CNR)

TR [msec] / TE [msec] / FA [deg]	49/40/20
FOV [mm]	220
Bandwidth [Px/Hz]	80
Parallel Imaging	GRAPPA-2
Average	1
No. of slices per MIP	8
Sliding Window	on

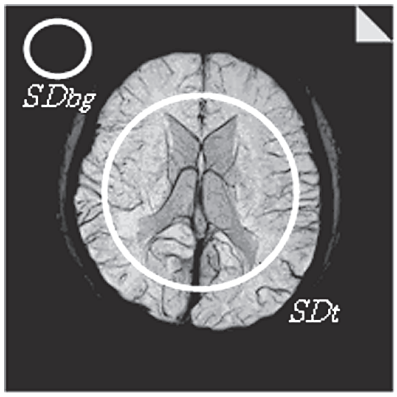

$$CNR = \sqrt{\frac{(SDt)^2 - (SDbg)^2}{(SDbg)^2}}$$

SDt: Standard deviation of tissue signal
SDbg: Standard deviation of background signal

Fig. 2 Calculation of the CNR by the total tissue method.

in Table 1. For images acquired under different conditions, the contrast-to-noise ratio (CNR) was calculated using the total tissue method (Fig. 2).

Then, 5 conditions were extracted based on consideration of the following: scan time, CNR, and SWI characteristics. Twelve healthy volunteers (age range, 22 to 38 years; average age, 28.8 years) were scanned under these conditions, and the acquired images were evaluated by 3 radiologists in a blinded manner. The images were evaluated in terms of visualization of the following structures: the internal cerebral veins, the vein of the caudate nucleus, the lateral vein of the lateral ventricle, and the cortical veins. The conditions were then ranked by the three radiologists on a scale of 1 to 5 points (range: poor conditions, 1 point - excellent conditions, 5 points) with respect to the quality of the susceptibility-weighted images. Kendall's coefficient of concordance was used for the statistical analysis.

Image processing conditions. The image processing conditions for SWI were investigated in terms of the following 2 parameters.

• Number of slices per MIP (number of slices to be combined in minIP)

• Sliding Window on/off (whether or not images were overlapped for display)

One of the healthy volunteers (26-year-old male) was scanned by SWI with the number of slices per MIP varying from 2 to 10, and with the Sliding Window set to "on" or "off" for each number of slices per MIP. The effect of each parameter setting was then evaluated. The scan parameters shown in Table 2 were employed, and evaluation was based on the following 4 items: i) visualization of the veins, ii) visualization of the red nucleus and substantia nigra, iii) influence of susceptibility artifacts, and iv) number of veins visualized per image.

Table 2 Scan parameters (visual evaluation)

TR [msec] / TE [msec] / FA [deg]	49/40/20
Thickness [mm]	2.0
Matrix	320×320
FOV [mm]	220
Bandwidth [Px/Hz]	80
Parallel Imaging	GRAPPA-2
Average	1

Results

Physical evaluation based on CNR. Table 3 shows the CNR values of images acquired with different slice thicknesses and matrix sizes. We avoided referring to the maximum and minimum values because data for only a single subject were obtained; however, the results suggested that the CNR value tended to increase with increasing slice thickness and decreasing matrix size.

Visual evaluation. Fig. 3 shows the results of visual evaluation for the 5 conditions that were extracted based on Table 3. The factors considered for the selection of conditions are described in greater detail below. Briefly, the factors were selected while taking scan time and SWI characteristics into consideration.

As regards the visual evaluation, the following scores were obtained: 3.31 for 2 mm/320 × 320, 3.47 for 3 mm/320 × 320, 4.47 for 3 mm/448 × 448,

Table 3 Comparison of CNR values with different acquisition conditions

CNR	1.0 mm	2.0 mm	3.0 mm	4.0 mm	5.0 mm
256×256	54.6	117.0	208.2	156.9	173.6
320×320	48.4	70.4	137.2	109.0	104.7
384×384	68.7	99.9	97.1	97.4	102.4
448×448	35.4	43.4	74.3	75.2	85.2
512×512	37.4	60.3	47.5	65.7	74.4

The CNR tends to be higher for thicker slices and smaller matrix sizes.

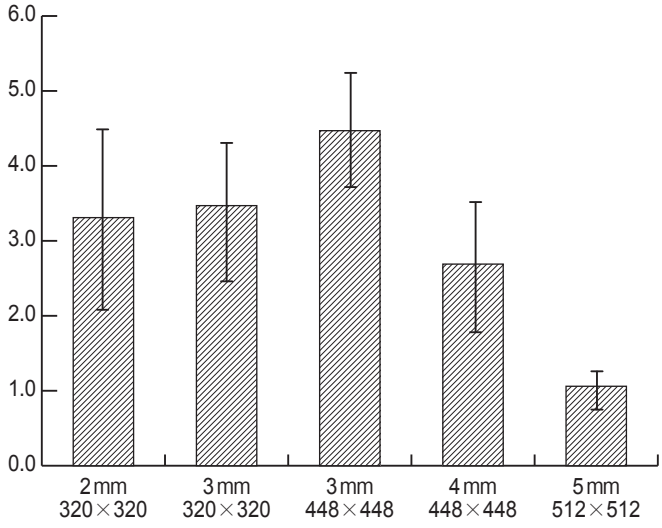

Fig. 3 Results of visual evaluation. Kendall's coefficient of concordance w = 0.89 was obtained in the statistical analysis.

2.69 for 4 mm/448 × 448, and 1.06 for 5 mm/512 × 512. The combination of a slice thickness of 3 mm and a matrix size of 448 × 448 achieved the highest score on the visual evaluation, with a Kendall's coefficient of concordance of w = 0.89 in the statistical analysis.

Image processing conditions. The effects of changing the number of slices per MIP and setting the Sliding Window on or off on images are shown in Table 4 and Fig. 4 respectively. Reducing the number of slices per MIP resulted in improvements in the three-dimensional visualization of vascular structures, and the visualization capabilities at the level of the posterior cranial fossa, as well as yielded a reduction in susceptibility artifacts. Increasing the number of slices per MIP, albeit at only the lateral-vein level, rendered it possible to obtain more information about the veins in a single image, thus improving the two-dimensional visualization of the veins. This approach was significantly affected by susceptibility artifacts at the level of the posterior cranial fossa; however, increasing the number of slices per MIP at the level of the lateral vein, appeared to be of advantage, as there are no structures in this region causative of susceptibility artifacts.

The results of the Sliding Window series demonstrated that this toggle (on/off) function is useful for visualizing the course of veins. Moreover, the utility of the Sliding Window function was further enhanced when the number of slices per MIP was increased.

Discussion

As discussed above, a susceptibility-weighted image is obtained by multiplication of the magnitude

Table 4 Influence on images of various numbers of slices/MIP and Sliding Window set to on or off

	No of slices per MIP				
	2	4	6	8	10
Visualization of course of veins	good	⟷	⟷	⟷	poor
Visualization of red nucleus and substantia nigra	good	⟷	⟷	⟷	poor
Influence of susceptibility artifacts	mild	⟷	⟷	⟷	severe
Number of veins visualized per image	poor	⟷	⟷	⟷	good
Usefulness of Sliding Window	low	⟷	⟷	⟷	high

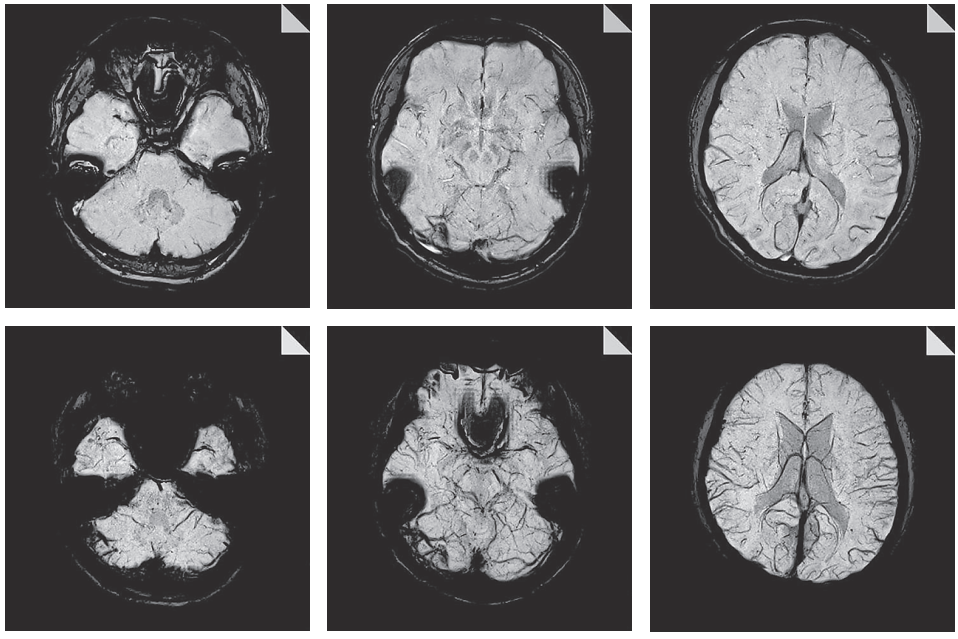

Fig. 4 Effect on images of various numbers of slices/MIP. The images in the top row were acquired with the number of slices per MIP set to 2, and the images in the bottom row were acquired with the number of slices per MIP set to 8. The settings affected susceptibility artifacts and visualization of veins.

image by the phase mask image that is generated from the phase image; as a result, differences in susceptibility are displayed as differences in image contrast. Data have been reported suggesting that certain parameters influence contrast in SWIs; among these parameters are the optimal TE and phase masking number (*i.e.*, the number of times the magnitude image is multiplied by the mask image) [1]. Since TE is proportional to the phase difference, the phase difference is more strongly enhanced with a long TE (equation 1). The phase difference is also enhanced when the phase masking number is increased (equation 2) [1, 3].

$$\varphi = -\gamma \cdot \Delta B \cdot TE \qquad \text{(equation 1)}$$

$$\rho_{SWI} = \rho_{magnitude} \cdot [\varphi_{mask}]^n \qquad \text{(equation 2)}$$

(n: Number of multiplications)

On the other hand, it is known that SWI is suitable for high-resolution acquisition because objects as small as one quarter of an acquisition voxel are visible in phase images in which the susceptibility effect is enhanced. However, with a 1.5-T system, high-resolution acquisition results in a reduction in the signal-

to-noise ratio (SNR), and the slice thickness, matrix size, and scan time must therefore be taken into consideration when determining the optimal acquisition conditions for SWI.

Two image processing conditions that affect susceptibility-weighted images are 1) the number of slices per MIP and 2) setting the Sliding Window to "on" or "off". The number of slices per MIP specifies the number of image slices to be combined for minIP image display. The Sliding Window is an application that overlaps the image slices to be displayed. When this application is set to "on", images in which the display slice thickness is determined by the number of slices per MIP are displayed by sliding the slice by the acquisition slice thickness. Images are displayed by acquisition slice thickness is 2 mm and the number of slices per MIP is 8, the thickness of the displayed image is 16 mm. When Sliding Window is set to "off", the acquisition range is simply displayed every 16 mm. When Sliding Window is set to on, the slice is shifted by 2 mm while a display slice thickness of 16 mm is maintained. In SWI, such image processing, including minIP, is performed at the time of image reconstruction, and not during post-processing at a workstation. As a result, in order to process images under different conditions for the evaluation of different types of lesions, the number of slices per MIP and the Sliding Window on/off function must be set prior to data acquisition. Taking these factors in consideration, the optimal conditions for SWI are discussed below.

Physical evaluation based on CNR measurements. The results of the CNR measurements revealed that the CNR value tends to increase with increase in slice thickness and decreases in matrix size. However, when an image with a relatively high CNR is visually compared to an image with a relatively low CNR, the image with the lower CNR is clearly superior as a susceptibility-weighted image, demonstrating that the CNR level does not necessarily reflect the quality of the susceptibility-weighted images (Fig. 5).

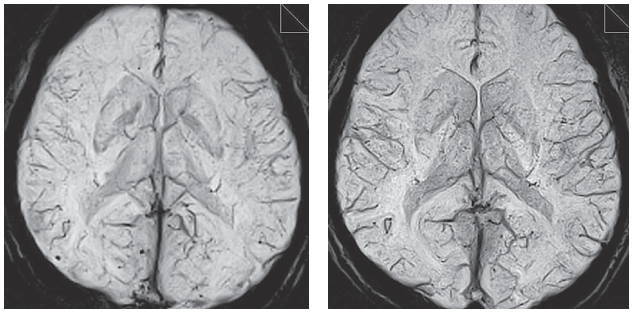

Fig. 5 Comparison of susceptibility-weighted images obtained with different CNR values. The CNR of the image on the left is 156.9 and the CNR of the image on the right is 70.4. Compared with the image on the left, the image on the right shows a lower CNR but superior visualization.

This finding is thought to be attributable to the fact that the signal levels of veins, hemorrhage, and ferrugination (*i.e.*, the targets to be visualized by SWI) are similar to the noise signal level [7–10]. CNR values are basically obtained from differences between tissue signals and the background noise signals (equation 3).

$$CNR = \frac{SIa - SIb}{SDair} \qquad \text{(equation 3)}$$

SI: Signal intensity, *SD*: Standard deviation

When a region of interest (ROI) is set in the cerebral parenchyma and another ROI is set in a vein and the signal intensities of both are measured, the signal of the vein is at the same level as that of the noise, and the signal intensity is close to zero. The calculated CNR is therefore highly dependent on the signal intensity of the cerebral parenchyma. In other words, CNR values are higher in scans performed using the conditions employed for obtaining a higher SNR in the cerebral parenchyma (thick slices, low resolution). The total tissue method was used for the CNR measurements in the present study, because use of the method in which a very small ROI is placed in a vein would have resulted in a significant measurement error; however, the results may be comparable using either method. Although imaging conditions providing higher resolution render it possible to visualize veins, hemorrhage, and ferrugination in greater detail, such conditions unfortunately also increase the noise components. Noise in the cerebral parenchyma signal itself also increases as a matter of course, resulting in a lower CNR. However, even when these factors are taken into consideration, the CNR does not reflect the quality of susceptibility-weighted images. As a consequence, we concluded that in the present study, the results of physical evaluation based on CNR measurements lacked validity. It will therefore be necessary to completely re-examine the physical evaluation

of SWI, starting with the evaluation method.

Visual evaluation. Since the results of physical evaluation based on the CNR lacked validity as described above, the acquisition conditions for visual evaluation were extracted from the perspective of selecting the appropriate scan time and high resolution using a CNR close to the recommended value. The scan time was set to less than 6 min, as the examination time is limited to 30 min at our institution and because SWI scanning is considered as an additional component of a routine examination. The acquisition conditions for obtaining as high a resolution as possible within the specified scan time were extracted because SWI is considered suitable for high-resolution acquisition.

In this series, slice thicknesses of 2 mm and 3 mm achieved high scores. In particular, the combination of a slice thickness of 3 mm and a matrix size of 320 × 320 was rated highly, even with relatively low-resolution imaging. On the other hand, the combination of a slice thickness of 5 mm and a matrix size of 512 × 512, which provides high resolution, was rated the lowest of the conditions tested. One explanation for this low rating could have been the low CNR. The significant reduction in the CNR, despite the thicker slice setting, suggested that a matrix size of 512 × 512 is not practical when a 1.5-T system is employed. Another possible reason for the low rating could be due to partial-volume effects. A thinner slice thickness provides higher image quality, but with the trade-off of a longer scan time, while a thicker slice thickness suffers from more severe partial-volume effects, resulting in poorer visualization capabilities. In addition, SWI is inherently susceptible to partial-volume effects because it employs phase images [1, 3, 11]. Based on the above considerations, it is thought that the partial-volume effects due to the use of a thicker slice setting had a greater influence than the higher resolution provided by a larger matrix size. The most important reason for poorer visualization capabilities in scans with a combination of a slice thickness of 5 mm and a matrix size of 512 × 512 is related to the fact that slices are combined in minIP processing. When minIP is performed, the thickness of the slice to be displayed is equal to the following: [acquisition slice thickness] × [number of slices per MIP]. When data are acquired at a slice thickness of 4 mm, for example, the display slice thickness is 8 mm, even if

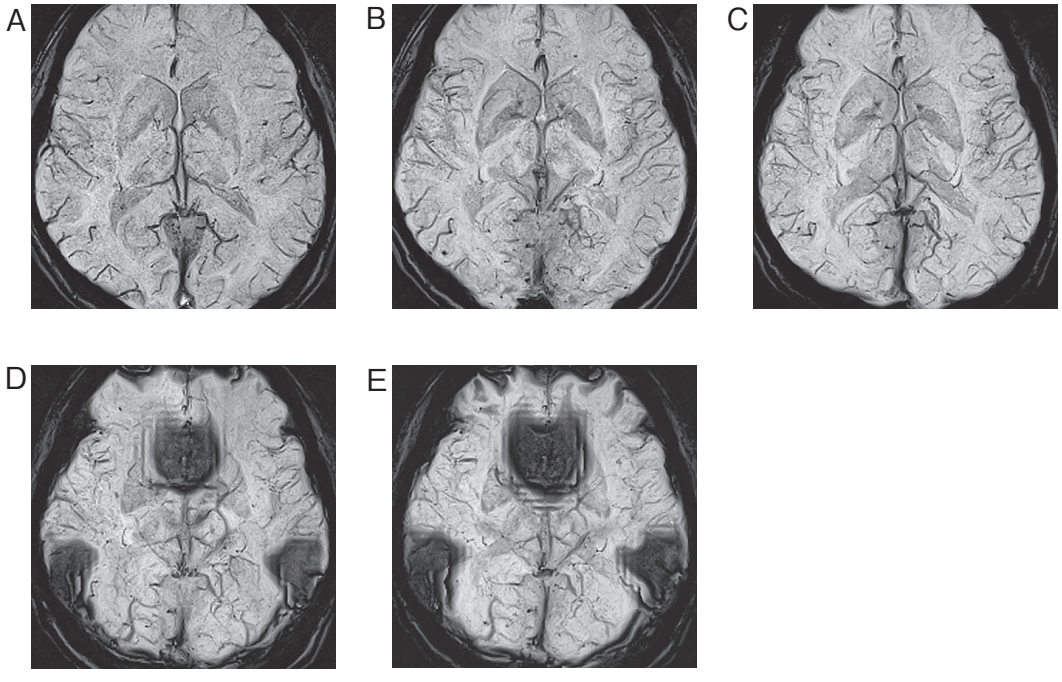

Fig. 6 Comparison of images acquired with different slice thicknesses: **A** = 1 mm, **B** = 2 mm, **C** = 3 mm, **D** = 4 mm, and **E** = 5 mm. The number of slices per MIP was set to 8. Susceptibility artifacts were increased and visualization was reduced as slice thickness increased.

the number of slices per MIP is set to a minimum value of 2. With acquisition at a slice thickness of 4 mm or 5 mm, the image is displayed as a thick slice after minIP processing, and is likely to contain more severe susceptibility artifacts at the level of the posterior cranial fossa. As a result, the partial-volume effects and susceptibility artifacts synergistically degrade the visualization capabilities in SWI. Fig. 6 shows images acquired with different acquisition slice thicknesses; here, the susceptibility artifacts are clearly increased and the visualization capabilities for the veins are reduced as the slice thickness is increased.

In the visual evaluation, the combination of a slice thickness of 3 mm and a matrix size of 448×448 was determined to be optimal when the limited scan time and the requirement for an isotropic pixel matrix were taken into consideration. However, the acceptable scan time differs among institutions, and the matrix does not necessarily need to provide isotropic pixels. It appears to be useful to set a thin slice thickness and to compensate for the longer scan time due to the larger number of partitions by reducing the matrix size in the phase-encode direction. Indeed, the default acquisition conditions are typically set in this manner. The results of the present study of image acquisition conditions can therefore be used as reference data for acquisition with an isotropic pixel matrix.

Image processing conditions. The results shown in Table 4 indicate that setting a minimum value of 2 for the number of slices per MIP is useful in terms of three of the four items for evaluation. For depicting the course of veins, the number of veins visualized in a single image increases when a larger number of slices are combined, and setting a larger number of slices per MIP is therefore advantageous for evaluating the course of veins in two-dimensional images. However, advantage of setting a larger number of slices per MIP is limited to slices at the level of the lateral ventricle. Slices at the level of the posterior cranial fossa and the vertex are likely to be affected by susceptibility artifacts, and the visualization capabilities in these peripheral slices are insufficient. If the acquisition slice thickness is set to 2 mm and the number of slices per MIP is set to 8, each slice displayed contains information for a thickness of 16 mm. Thickness renders it difficult to observe the course of veins in the appropriate slice direction. Based on these considerations, the number of slices per MIP should be set to the smallest value possible in order to obtain high-quality susceptibility-weighted images, even at the level of the posterior cranial fossa and the vertex; this approach would also facilitate observation of the course of veins in the slice direction.

Moreover, as regards visualization of the red nucleus and substantia nigra, it was found that the selection of a smaller number of slices per MIP yielded more favorable results. Fig. 7 shows differences in visualization for different numbers of slices per MIP in the same slice. The visualization capabilities with respect to the red nucleus and substantia nigra were clearly reduced with increases in the number of slices per MIP, because when a larger number of slices are combined, data from a number of slices are displayed together, and local visualization capabilities are therefore impaired.

As regards evaluation of the influence of susceptibility artifacts, the use of a smaller number of slices per MIP was again considered more beneficial. In SWI, the contrast between tissues with different susceptibilities is enhanced, and veins, hemorrhage, and ferrugination are clearly depicted [1, 3]. In other words, susceptibility-weighted images are more strongly affected by changes in susceptibility than are standard images. This is especially pronounced at the level of the posterior cranial fossa, as shown in Fig. 8, which shows a $T2^*$-weighted image (as has conventionally been used as a susceptibility-weighted image [12]) and a susceptibility-weighted image. The influence of susceptibility artifacts is increased even further when the number of slices to be combined increases. Furthermore, when the number of slices to be combined is increased, the displayed slice becomes thicker and contains more severe susceptibility artifacts, especially at the level of the posterior cranial fossa. Based on these considerations, the number of slices per MIP should be set to the minimum value in order to minimize the influence of susceptibility artifacts.

The relationship between the usefulness of the Sliding Window and the number of slices per MIP was also evaluated. As stated above, the Sliding Window is an application in which image slices are overlapped for display. The evaluation results showed that this application is more useful when the number of slices

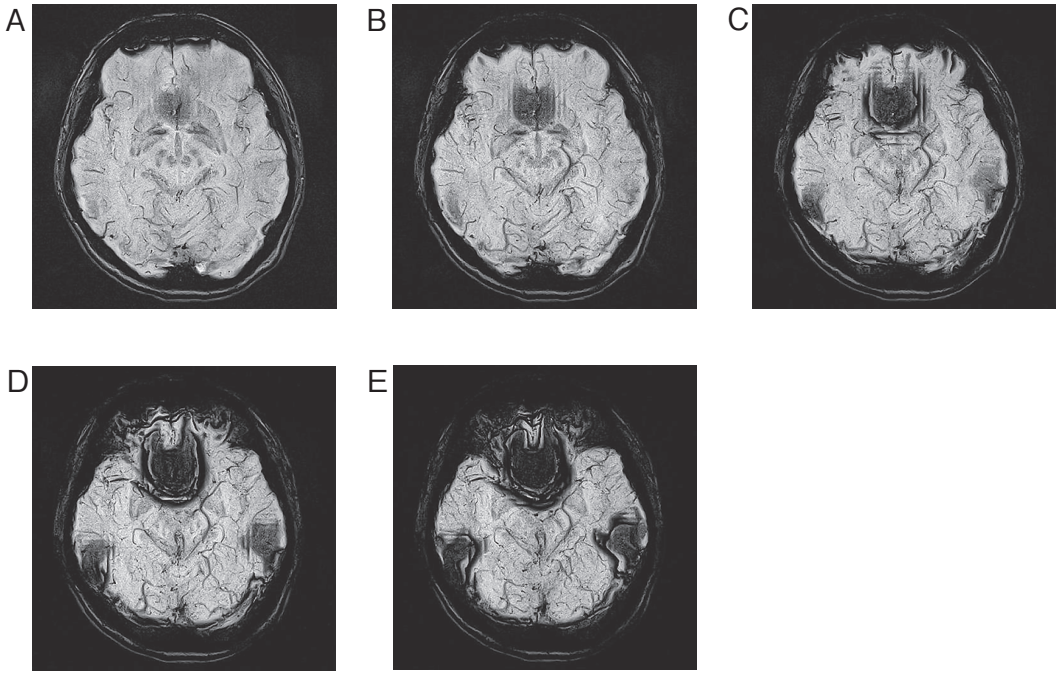

Fig. 7 Comparison of images acquired with different numbers of slices per MIP: **A** = 2, **B** = 4, C = 6, **D** = 8, and **E** = 10. The visualization of the red nucleus and substantia nigra was increasingly impaired with increases in the number of slices per MIP.

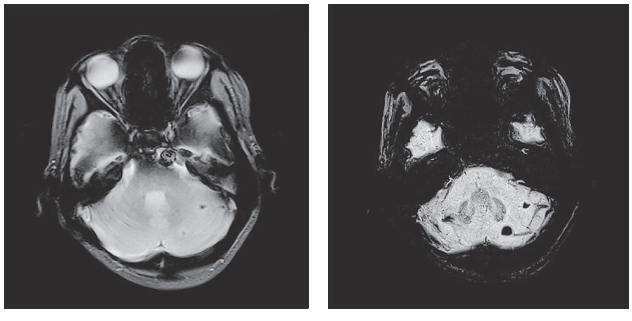

Fig. 8 Comparison of susceptibility artifacts at the level of the posterior cranial fossa. The image on the left was acquired by T2*-weighted imaging and the image on the right was acquired by SWI. The artifact-inducing influence of bones was more pronounced in the susceptibility-weighted image.

Table 5 Number of images displayed with Sliding Window on or off

Number of slices per MIP	2	8
Scan range	120 mm	
Acquisition slice thickness	2.0 mm	
Display slice thickness	4.0 mm	16.0 mm
Number of images displayed (Sliding Window = on)	59	53
Number of images displayed (Sliding Window = off)	30	8

per MIP is large. The Sliding Window is advantageous for observing the course of veins, and this advantage remains unaffected by the acquisition conditions. When the Sliding Window is set to "on", images can be paged by the acquisition slice thickness, rather than by the slice thickness after minIP. The difference between the acquisition slice thickness and the display slice thickness is relatively small with a decreasing slice number/MIP, but the difference increases with increases in the number of slices per MIP. Table 5 shows the number of images displayed with different numbers of slices per MIP. It is to be expected that more detailed information can be obtained when a larger number of images are displayed, as long as the scanning range and the acquisition conditions are identical. Accordingly, the Sliding Window function is more useful with larger differences between the acquisition slice thickness and the display slice thickness, *i.e.*, with larger numbers of

slices per MIP.

Based on the results obtained for the image processing conditions evaluated here, it was generally concluded that a minimum of 2 slices per MIP should be selected and the Sliding Window should be on. However, the type of information required differs among institutions, as do the acquisition conditions, and these conditions require additional minor adjustments dependent on the slice thickness setting. Whether diagnosis is performed based on images displayed on a monitor or images printed out on film is another factor that must be taken into consideration during parameter setting. It is hoped that the results of the present evaluation of processing conditions will provide useful reference data, and that the influence of scan parameters on images as discussed here will be taken into consideration.

Conclusions. The present study provides basic data concerning acquisition and image processing conditions that may in certain cases be useful for setting standards for optimizing SWI sequences. Further investigation of the physical evaluation of susceptibility-weighted images will still be necessary.

References

1. Haacke EM, Xu Y, Cheng YC and Reichenbach JR: Susceptibility weighted imaging (SWI). Magn Reson Med (2004) 52: 612–618.
2. Rauscher A, Sedlacik J, Barth M, Haacke EM and Reichenbach JR: Noninvasive assessment of vascular architecture and function during modulated blood oxygenation using susceptibility weighted magnetic resonance imaging. Magn Reson Med (2005) 54: 87–95.
3. Sehgal V, Delproposto Z, Haacke EM, Tong KA, Wycliffe N, Kido DK, Xu Y, Neelavalli J, Haddar D and Reichenbach JR: Clinical applications of neuroimaging with susceptibility-weighted imaging. J Magn Reson Imaging (2005) 22: 439–450.
4. Lee BC, Vo KD, Kido DK, Mukherjee P, Reichenbach J, Lin W, Yoon MS and Haacke M: MR high-resolution blood oxygenation level-dependent venography of occult (low-flow) vascular lesions. AJNR Am J Neuroradiol (1999) 20: 1239–1242.
5. Reichenbach JR, Jonetz-Mentzel L, Fitzek C, Haacke EM, Kido DK, Lee BC and Kaiser WA: High-resolution blood oxygen-level dependent MR venography (HRBV): a new technique. Neuroradiology (2001) 43: 364–369.
6. Ida M, Motoyoshi K, Yoshisawa H, Hino K, Mizuuchi N, Maruyama K, Yoshida M, Kitahara K and Fukuda K: Susceptibility-weighted imaging (SWI): A Novel imaging using phase contrast. Neuro Ophthalmol Jpn (2006) 23: 283–289 (in Japanese).
7. Reichenbach JP, Venkatesan R, Yablonskiy DA, Thompson MR, Lai S and Haacke EM: Theory and application of static field inhomogeneity effects in gradient-echo imaging. J Magn Reson Imaging (1997) 7: 266–279.
8. Thulborn KR, Waterton JC, Matthews PM and Radda GK: Oxygenation dependence of the transverse relaxation time of water protons in whole blood at high field. Biochim Biophys Acta (1982) 714: 265–270.
9. Li D, Waight DJ and Wang Y: In vivo correlation between blood T2* and oxygen saturation. J Magn Reson Imaging (1998) 8: 1236–1239.
10. Haacke EM, Cheng NY, House MJ, Liu Q, Neelavalli J, Ogg RJ, Khan A, Ayaz M, Kirsch W and Obenaus A: Imaging iron stores in the brain using magnetic resonance imaging. Magn Reson Imaging (2005) 23: 1–25.
11. Cheng YCN and Haacke EM: Predicting BOLD signal changes as a function of blood volume fraction and resolution. NMR Biomed (2001) 14: 468–477.
12. Kato H, Izumiyama M, Izumiyama K, Takahashi A and Itoyama Y: Silent cerebral microbleeds on T2*-weighted MRI: correlation with stroke subtype, stroke recurrence, and leukoaraiosis. Stroke (2002) 33: 1536–1540.